

Challenge of Magnetism in Strongly Correlated Open-Shell $2p$ Systems

Jürgen Winterlik,¹ Gerhard H. Fecher,¹ Catherine A. Jenkins,¹ Claudia Felser,¹ Claus Mühle,² Klaus Doll,² Martin Jansen,² Leonid M. Sandratskii,³ and Jürgen Kübler⁴

¹*Institut für Anorganische und Analytische Chemie, Johannes Gutenberg-Universität, D-55099 Mainz, Germany*

²*Max-Planck-Institute for Solid State Research, 70569 Stuttgart, Germany*

³*Max-Planck-Institute of Microstructure Physics, 06120 Halle, Germany*

⁴*Institute for Solid State Physics, Technische Universität, 64289 Darmstadt, Germany*

(Received 11 June 2008; published 5 January 2009)

We report on theoretical investigations of the exotic magnetism in rubidium sesquioxide Rb_4O_6 , a model correlated system with an open $2p$ shell. Experimental investigations indicated that Rb_4O_6 is a magnetically frustrated insulator. The frustration is explained here by electronic structure calculations that incorporate the correlation between the oxygen $2p$ electrons and deal with the mixed-valent oxygen. This leads to a physical picture where the symmetry is reduced because one third of the oxygen in Rb_4O_6 is nonmagnetic while the remaining two thirds assemble in antiferromagnetic arrangements. A degenerate, insulating ground state with a large number of frustrated noncollinear magnetic configurations is confidently deduced from the theoretical point of view. These findings demonstrate in general the importance of electron-electron correlations in open-shell p -electron systems.

DOI: 10.1103/PhysRevLett.102.016401

PACS numbers: 71.20.Be, 68.47.Gh, 75.50.-y

Solid oxygen is the paradigm for p -electron-based magnetic ordering in compounds and is, together with NO, the only molecular crystal that carries a magnetic moment. It exhibits an antiferromagnetic (AFM) transition at a Néel temperature of 24 K [1], and with moderate pressure, planes in the AFM solid couple ferromagnetically [2]. With higher pressure the molecular crystal becomes metallic [3] and then superconducting [4].

The alkali-metal oxides constitute an intermediate step on the way from molecular oxygen to the ionic transition-metal oxides. The alkali-metal atoms transfer their electrons to the oxygen molecules resulting in ionic crystals with dioxygen anions that retain the molecular properties of solid oxygen [5]. In particular, the heavy alkali metals form compounds with oxidation states that range from metallic suboxides [6] to the ozonides [7]. In this Letter it will be shown that the alkali sesquioxides— Rb_4O_6 and Cs_4O_6 —are of principal importance. Since these compounds are open-shell $2p$ systems within a solid, quantum chemistry and condensed matter meet in an intriguing fashion.

The black color of Rb_4O_6 suggests that it has an unconventional electronic structure, since comparable alkali hyperoxides or peroxides are pale yellow or white. Rb_4O_6 is an insulator with a resistivity of approximately $0.04 \text{ M}\Omega \text{ m}$ [8]. The sesquioxide contains three dioxygen anions with two possible valencies: the closed-shell peroxide anion O_2^{2-} and the open-shell hyperoxide anion O_2^- . The hyperoxide corresponds to a charged oxygen molecule (radical) and localizes its single unpaired electron in an antibonding π^* orbital. This causes the rare phenomenon of anionogenic magnetic order. Anionogenic magnetism is also observed, for example, in rubidium hyperoxide RbO_2 , an insulating antiferromagnet with a Néel temperature of 15 K

[9]. Electronic structure calculations have been used to predict *half-metallic ferromagnetism* in canonical open-shell $2p$ systems such as nanographene [10] or hole-doped MgO [11]. Similar predictions were made for Rb_4O_6 [12], but the underlying calculations failed to give an accurate description of its insulating and magnetic properties.

Rubidium sesquioxide crystallizes in the Pu_2C_3 structure type. Inelastic neutron scattering studies confirmed the simultaneous presence of O_2^- and O_2^{2-} anions [13]. Magnetization measurements [14] indicate a complicated electronic structure with a magnetic transition at approximately 3.4 K. An effective magnetic moment of $m = 1.83\mu_B$ per hyperoxide anion was deduced from a Curie-Weiss fit. Thermal irreversibilities were observed between zero-field-cooled (ZFC) and field-cooled (FC) magnetization measurements. These phenomena are specific to spin glasses and related random magnetic systems [15,16]. Further experiments indicated that the magnetization of Rb_4O_6 shows a dynamic time dependent behavior below the magnetic transition [8]. The magnetization as a function of time follows an exponential law with a relaxation time of $\tau = (1852 \pm 30) \text{ s}$. Magnetic and geometric frustration are observed frequently in d -electron systems such as the spinel LiV_2O_4 [17] or the cubic vanadates [18]. In Rb_4O_6 , however, the magnetic moment is carried by the p electrons of the anionic hyperoxide molecules. Here we show for the first time that open-shell $2p$ compounds exhibit magnetic frustration and behave like other correlated d - or f -electron systems.

For a detailed analysis of the electronic and magnetic structures of Rb_4O_6 , its crystal structure must be understood. Figure 1(a) shows a body-centered cubic unit cell of Rb_4O_6 . It contains 12 dioxygen anions that are distinguished by their valency and their alignment along the

principal axes. The experimental bond lengths for the hyperoxide and the peroxide anions are approximately $0.14a$ and $0.17a$, respectively. The cubic lattice parameter is approximately $a \approx (9.2-9.3)$ Å depending on the temperature [19,20]. The next-nearest-neighbor environment of one hyperoxide anion is highlighted in Fig. 1(b). The arrows denote the total molecular moment in an arrangement justified below. An AFM configuration that satisfies all interactions between hyperoxide anions is impossible; the order is frustrated.

Electronic structure calculations of Rb_4O_6 were performed using the quantum chemical CRYSTAL code [21] (details of the calculations are summarized in Ref. [22]). The implementation of the *exact exchange* Becke three-parameter Lee-Yang-Parr (B3LYP) hybrid functional [23] makes it useful for the theoretical treatment of molecular systems with a high degree of electron localization. A full optimization of the fractional coordinates was performed assuming that the dioxygen anions remain ferromagnetically ordered. A metallic ground state was obtained with space group $I\bar{4}3d$ where all dioxygen anions are symmetrically equivalent. The structural optimization resulted in a structure with lower symmetry (space group $I\bar{4}2d$) and different bond lengths of the peroxide and hyperoxide anions. Using the exact exchange hybrid functional, it converged to an insulating state as shown in Fig. 1(a), where *all* peroxide anions are aligned along a single axis. The optimized bond lengths of $0.146a$ for the hyperoxides and $0.167a$ for the peroxides are in good agreement with the experimental values. The observed magnetic frustration cannot be calculated using the CRYSTAL code. Pure local density approximation (LDA) calculations result,

however, in a metallic state [12], which is in disagreement with the experiments [8]. To overcome these difficulties, the augmented spherical wave (ASW) method [24] together with LDA plus the multiorbital mean-field Hubbard model LDA + U [25] was used to explain both the magnetic frustration and the insulating state (for details see Ref. [22]). The LDA + U method treats electron-electron correlations in narrow bands quite accurately in a mean-field sense. The Hubbard parameter U was implemented into the ASW code allowing for unrestricted non-collinear moment arrangements [26]. In the double counting correction scheme used here, the results depend only on the difference between U and the exchange parameter J . For simplicity, this difference is denoted by U in the following. A meaningful choice of U is not obvious *a priori*, but a discussion of possible values for oxygen in Ref. [27] and the experimentally determined large resistivity [8] suggest that values around 6 eV are a good choice.

The ASW LDA + U calculations converged only if the different bond lengths of the hyperoxide and peroxide pairs are accounted for. This is in agreement with the results of the cell optimization by CRYSTAL. The peroxide anions are chosen to be aligned along a single axis and found to be nonmagnetic. The hyperoxide anions are aligned along the orthogonal axes and couple antiferromagnetically with a magnetic moment of approximately $1\mu_B$ per pair [Fig. 1(b)]. This accumulated moment does not depend on the choice of the parameter U . The individual contributions to the total moment, however, diverge from the original value of $0.5\mu_B$ as U increases. The symmetry is thus further reduced. The choice of axis for the peroxide anions is symmetrically equivalent, so it is assumed that the system spontaneously chooses an orientation for the peroxide anions that leads to antiferromagnetic order of the hyperoxide anions aligned along the perpendicular directions. Thus, the antiferromagnetism is degenerate and the peroxide anion is chosen to lie along the z axis for all the following calculations.

Figures 2(a) and 2(b) show sections of the spin-resolved density of states in the vicinity of the Fermi energy for antiferromagnetic configurations using $U = 4.1$ eV and $U = 8.2$ eV. For these values, the gap that separates the occupied from the empty states is $E_G \approx 0.1$ eV in 2(a) and $E_G = 0.8$ eV in 2(b). An intermediate value for the effective Hubbard parameter of $U = 6.8$ eV results in $E_G = 0.5$ eV (not shown). In all cases, a complete charge separation is obtained for the peroxide and hyperoxide anions. The magnetic moments of the peroxide anion are strictly zero. The highest occupied states are localized at the nonmagnetic peroxide anions. The s density originates from the Rb ions and supplies the bonding and exchange paths.

For comparison, Fig. 2(a) exhibits the density of states in the ferromagnetic configuration obtained by CRYSTAL. The electronic structure is obviously insulating. The gap emerges from the splitting of the O_2^- and O_2^{2-} $pp\pi$

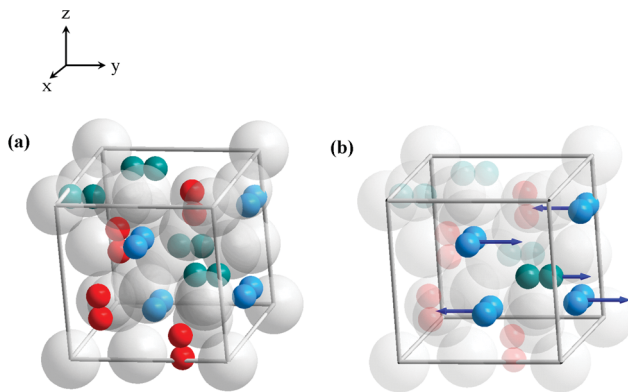


FIG. 1 (color). The pseudo-body-centered cubic cell of Rb_4O_6 is depicted in (a). Differently oriented dioxygen anions are drawn with different colors so that the alignment along the axes can be distinguished. For clarity, the Rb atoms are gray and transparent. The nonmagnetic peroxide anions (red) are assumed to be aligned along the z axis. The next-nearest-neighbor environment of one molecule consisting of hyperoxide anions is highlighted in (b). The vectors represent the total magnetic moment of an anion. The order is that found in the calculations.

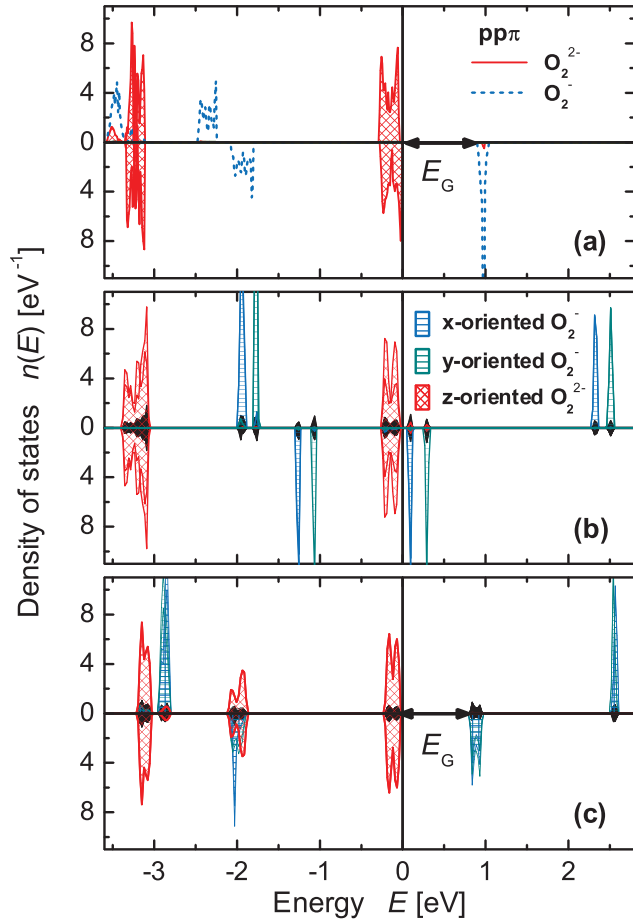


FIG. 2 (color). The density of states for Rb_4O_6 obtained by CRYSTAL with the exact exchange hybrid functional for a ferromagnetic configuration of the O_2^{2-} anions is shown in (a). (b), (c) show the sublattice density of states obtained by ASW with LDA + U for an antiferromagnetic setup [$U = 4.1$ eV (b) and $U = 8.1$ eV (c)]. Red shading is used for the nonmagnetic O_2^{2-} anions, blue and cyan for the magnetic O_2^{2-} anions. Black shading indicates Rb s states. The upper halves are spin-up; the lower halves spin-down. The energy origin is chosen to be the Fermi energy. The value of the energy gap E_G that separates the highest occupied states from the lowest unoccupied states is $E_G \approx 0.9$ eV in (a), 0.1 eV in (b), and 0.8 eV in (c).

orbitals. All $pp\sigma$ states are too far below the Fermi energy to affect the electronic character of Rb_4O_6 . Starting with a ferromagnetic configuration in the ASW calculations with values of U below 4.1 eV, the electronic structure became half-metallic ferromagnetic. At $U = 4.1$ eV a magnetic moment of exactly $4\mu_B$ per unit cell was obtained. The peroxide anions become weakly magnetic with an induced moment of $0.1\mu_B$, decreasing to $0.05\mu_B$ for the largest value of U . The ferromagnet became insulating for $U = 6.8$ and 8.2 eV.

The ferromagnet is now excluded from our consideration by using the total energy criterion. For $U = 4.1$ eV, it is 87 meV per unit cell higher for the ferromagnet relative

to the antiferromagnetic state. For even larger values of U , the stability of the antiferromagnetic state decreases slightly to approximately 56 meV per unit cell for $U = 8.1$ eV. It is thus the electron correlation that leads to an antiferromagnetic ground state, although it cannot be definitively asserted that the true ground state is exactly as depicted in Fig. 1(b).

It is nontrivial to find the true ground state out of the large number of possible noncollinear spin orientations. Spiral modulations of the antiferromagnet enable an improved search [26,28], provided that spin-orbit interaction can be neglected (as justified here [22]). A magnetic spiral is defined by the size of the magnetic moment, an angle of tilt θ , and a wave vector \mathbf{k} that can be chosen in the Brillouin zone of the crystal. For convenience, a tilt angle of $\theta = 90^\circ$ is used. Such a spin spiral changes the polar angle of the moment of the ion with basis vector \mathbf{x} by $\phi = \mathbf{2}(k \cdot \mathbf{x})$.

Spin spirals with various values of the wave vector \mathbf{k} are thus superimposed onto the antiferromagnetic state. Assuming the force theorem to be a good approximation, the total energy changes ΔE_{tot} for each value of \mathbf{k} are calculated. The resulting values of ΔE_{tot} are extremely small for \mathbf{k} along the [001] direction. The energy changes are shown in Fig. 3 for $U = 4.1, 6.8,$ and 8.1 eV. The spiral energies for any direction in the Brillouin zone other than [001] are larger by three to four orders of magnitude because the parallel coupling within the hyperoxide anion is extremely strong and the moments remain parallel only for \mathbf{k} along [001].

The frustration of the magnetic moments is clearly seen in the antiferromagnetic case [see Figs. 1(b) and 3] where the alternating ferromagnetic and antiferromagnetic bonds are obvious]. The magnetic moments along the next-nearest-neighbor connections are perpendicular for $\mathbf{k} = (0, 0, 1)$ at the zone boundary and are thus no longer frustrated. The flat and slightly negative portions of ΔE_{tot} for $U = 4.1$ and 6.8 eV may be assumed to serve as a reservoir of states to release the frustration, although it should be noticed that the part of k space available along [001] is extremely restricted.

A theoretical description of the electronic and magnetic state of the model alkali-metal oxide system Rb_4O_6 that is compatible with experimental results [8] is thus only possible by taking into account the electron-electron correlations, a complex magnetic arrangement of the spins, and the reduction of the symmetry. In particular, the existence of nonmagnetic peroxide anions is essential and results in a peculiar electronic texture in real and reciprocal space.

In summary, it has been shown that the proposed half-metallic ferromagnetism [12] in Rb_4O_6 is unrealistic, and instead an insulating ground state is obtained. The magnetic order is found to be quite exotic in so far as one third of the oxygen becomes nonmagnetic while the remaining two thirds assemble in a frustrated antiferromagnetic configuration. The magnetic frustration and the spin spiral

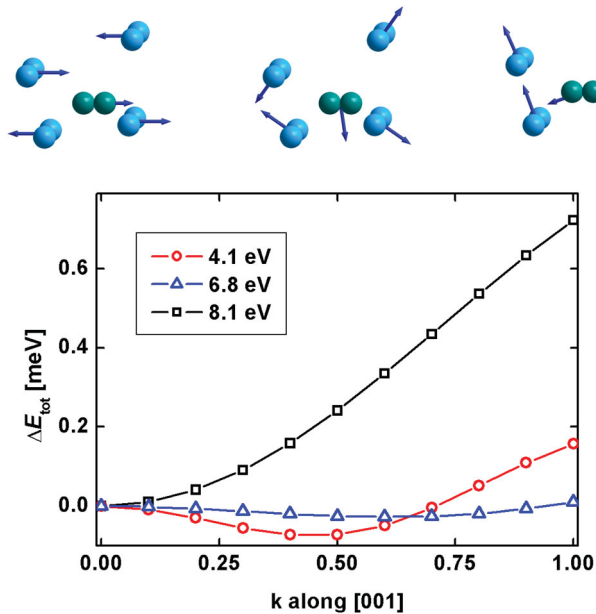


FIG. 3 (color). The line plot shows the spiral energies of antiferromagnetic Rb_4O_6 as functions of the spiral vector \mathbf{k} in units of $2\pi/a$ along the $[0, 0, 1]$ direction for $U = 4.1, 6.8,$ and 8.1 eV. The corresponding magnetic configurations are sketched for $k = 0$, $\mathbf{k} = (0, 0, 0.5)$, and $\mathbf{k} = (0, 0, 1)$. The energy is given per primitive cell.

state in Rb_4O_6 as well as its multidegenerate ground state were demonstrated using noncollinear spin calculations. The calculations explain both the strong time dependence of the magnetization and the pronounced differences between the ZFC and FC measurements that are characteristic of a frustrated magnetic state [8]. The frustration is of geometric origin and caused by the peculiar symmetry of Rb_4O_6 . The importance of electronic correlation in a $2p$ compound was demonstrated here for Rb_4O_6 . Open-shell $2p$ systems thus behave like $3d$ or $4f$ systems. Strong correlation is also expected to be important in other p -electron systems. In this Letter it was shown that Rb_4O_6 serves as a model for other open-shell systems that are based on p electrons.

This work was funded by the DFG in the Collaborative Research Center *Condensed Matter Systems with Variable Many-Body Interactions* (TRR 49). The authors are grateful for the fruitful discussions with W. Pickett, M. Jourdan, G. Jakob, and H. von Löhneysen.

- [1] R.J. Meier and R.B. Helmholdt, Phys. Rev. B **29**, 1387 (1984).
 [2] I.N. Goncharenko, O.L. Makarova, and L. Ulivi, Phys. Rev. Lett. **93**, 055502 (2004).

- [3] Y. Akahama, H. Kawamura, D. Häusermann, M. Hanfland, and O. Shimomura, Phys. Rev. Lett. **74**, 4690 (1995).
 [4] K. Shimizu, K. Suhara, M. Ikumo, M.I. Eremets, and K. Amaya, Nature (London) **393**, 767 (1998).
 [5] I. A. Nekrasov, M. A. Korotin, and V.I. Anisimov, arXiv: cond-mat/0009107v1.
 [6] A. Simon, Z. Anorg. Allg. Chem. **431**, 5 (1977).
 [7] M. Jansen and H. Nuss, Z. Anorg. Allg. Chem. **633**, 1307 (2007).
 [8] J. Winterlik, G.H. Fecher, C.A. Jenkins, C. Felser, J. Kübler, C. Mühle, K. Doll, M. Jansen, T. Palasyuk, M.I. Eremets, and F. Emmerling (unpublished).
 [9] M. Labhart, D. Raoux, W. Känzig, and M.A. Bösch, Phys. Rev. B **20**, 53 (1979).
 [10] Y.-W. Son, M.L. Cohen, and S.G. Louie, Nature (London) **444**, 347 (2006).
 [11] I.S. Elfimov, A. Rusydi, S.I. Csiszar, Z. Hu, H.H. Hsieh, H.-J. Lin, C.T. Chen, R. Liang, and G.A. Sawatzky, Phys. Rev. Lett. **98**, 137202 (2007).
 [12] J.J. Attema, G.A. de Wijs, G.R. Blake, and R.A. de Groot, J. Am. Chem. Soc. **127**, 16325 (2005).
 [13] M. Jansen, R. Hagenmayer, and N. Korber, C.R. Acad. Sci. Ser. 2c **2**, 591 (1999).
 [14] J. Winterlik, G.H. Fecher, C. Felser, C. Muehle, and M. Jansen, J. Am. Chem. Soc. **129**, 6990 (2007).
 [15] K. Binder and A.P. Young, Rev. Mod. Phys. **58**, 801 (1986).
 [16] A.P. Ramirez, Annu. Rev. Mater. Sci. **24**, 453 (1994).
 [17] C. Urano, M. Nohara, S. Kondo, F. Sakai, H. Takagi, T. Shiraki, and T. Okubo, Phys. Rev. Lett. **85**, 1052 (2000).
 [18] G. Khaliullin, P. Horsch, and A.M. Oles, Phys. Rev. Lett. **86**, 3879 (2001).
 [19] T. Bremm and M. Jansen, Z. Anorg. Allg. Chem. **610**, 64 (1992).
 [20] H. Seyeda and M. Jansen, J. Chem. Soc. Dalton Trans. 875 (1998).
 [21] R. Dovesi *et al.*, *CRYSTAL 2006 User's Manual* (University of Torino, Torino, 2006).
 [22] See EPAPS Document No. E-PRLTAO-102-007902 for details about the methodologies of the electronic structure calculations used in this work. For more information on EPAPS, see <http://www.aip.org/pubservs/epaps.html>.
 [23] A.D. Becke, J. Chem. Phys. **98**, 5648 (1993).
 [24] A.R. Williams, J. Kübler, and C.D. Gelatt, Phys. Rev. B **19**, 6094 (1979).
 [25] V.I. Anisimov, J. Zaanen, and O.K. Andersen, Phys. Rev. B **44**, 943 (1991).
 [26] M. Uhl, L.M. Sandratskii, and J. Kübler, Phys. Rev. B **50**, 291 (1994).
 [27] C. Cao, S. Hill, and H.-P. Cheng, Phys. Rev. Lett. **100**, 167206 (2008).
 [28] L.M. Sandratskii, Adv. Phys. **47**, 91 (1998).